

# BEAM TRANSVERSE SIZE EFFECTS IN THE OTR SPECTRUM AS A HIGH RESOLUTION DIAGNOSTIC TOOL

G.L. Orlandi\*, B. Beutner, R. Ischebeck, V. Schlott, B. Steffen  
Paul Scherrer Institut, 5232 Villigen PSI, Switzerland

## Abstract

Diagnostics with a transverse spatial resolution in the order or even higher than the intrinsic limit of the traditional OTR light spot imaging techniques is required for high energy and low emittance electron beams by FEL driver linac. High resolution measurements of the beam transverse size can be performed by moving the radiation detection from the space of the electron transverse coordinates to the Fourier conjugate space of the radiation angular distribution. The development of such a new diagnostic technique is related to the experimental investigation of the beam transverse size effects in the angular distribution of the OTR spectral intensity. The status of the experimental investigation of such a phenomenon at the SwissFEL project and the main features of such a new diagnostic technique will be presented.

## INTRODUCTION

Diagnostics for fourth generation light sources is required to monitor the beam transverse size with ever higher spatial resolution. Spatial resolutions from 10 to 5  $\mu\text{m}$  are indeed envisaged at the 250 MeV injector of the future SwissFEL [1]. OTR view screens (OTR, Optical Transition Radiation) appear suitable tools for monitoring high energy electron beams with small transverse size. Limitations to OTR monitor spatial resolution comes mainly from the detection set up (CCD camera and optical device). With decrease of the beam transverse size and increase of the beam energy, the traditional OTR imaging techniques in the space of the electron coordinates have to face the problem to spatially resolve a large flux of photons that concentrates in few pixels of the CCD sensor. How to overcome such an intrinsic spatial resolution limitation of the traditional OTR diagnostics? Having in mind the electron bunch length investigation from spectroscopic analysis of the temporal coherence in the transition or synchrotron radiation spectra, as the detection of a given radiation pulse is showing – in a given coordinate space – features of a narrow-band phenomenon, broad-band conditions for the investigation of the same phenomenon can be still achieved if the observation of it can be moved from the primitive coordinate space to the conjugate Fourier space. In the specific case of OTR diagnostics in a FEL driver linac, what the physical phenomenon allowing us to shift the investigation of the electron beam transverse size from the space of the electron coordinates to the conjugate Fourier space of the radiation angular distribution? Diffractive modifications of the OTR spectral and angular distribution due to the finite transverse

size of the electron beam are expected to make possible the investigation of the beam-transverse-size in the conjugate Fourier space of the electron coordinates. The experimental check of such a phenomenon and the development of the related diagnostic technique are presently under investigation at the SwissFEL project.

## PHENOMENOLOGICAL BACKGROUND

Based on an original development of the virtual quanta method for a three-dimensional electron beam, the formal expression of the transition radiation (TR) energy spectrum for a high density charged beam in collision at a normal angle of incidence with a plane metallic surface having an arbitrary shape and size was obtained in the framework of the Huygens-Fresnel principle under far-field approximation [3, 4, 5]. For observation conditions of both temporal coherence and incoherence, the angular distribution of the TR spectral intensity results to be affected by a high frequency diffractive cut-off due to the finite transverse size of the electron beam. Such a diffractive effect should manifest itself as an increase of the number of photons emitted at a given wavelength and a broadening of their angular distribution with decrease of the beam transverse size. Such a phenomenon shows a physical consistency compared to other beam-transverse-size effects characterizing, in general, the radiation emission by relativistic charged beams. Synchrotron radiation Brilliance in a storage ring or photon bremsstrahlung Luminosity in a positron electron collider are indeed well known and investigated beam-transverse-size dependent properties of the radiation emission by charged beams as well as diffractive alterations of the synchrotron radiation angular distribution in an electron storage ring are commonly investigated to monitor and optimize the beam transverse size [2]. Finally, it should be noticed that the collision of a charged beam with a flat metallic surface – in the present context normally oriented with respect to the colliding beam and supposed to behave as an ideal conductor – can be schematized as the collision of a relativistic charged beam with a double layer of charge at rest in the laboratory frame of reference. The backward and forward TR emitted during the collision is the result of the dipolar oscillation of the charge induced conduction electron on the metallic surface, as confirmed by the observation of backward emitted radiation. Consequently, from the point of view of kinematics, TR emission by a charged beam in collision with a normally oriented metallic surface can be assimilated to a photon bremsstrahlung emission by a relativistic charged beam colliding with a charged distribution at rest – along the direction of incidence – in the laboratory frame of reference. The tight relativistic ori-

\* gianluca.orlandi@psi.ch

gin and the common kinematic nature that TR shares with other electromagnetic radiative mechanisms by relativistic charged beams make the investigation of the beam transverse size effects on the TR energy spectrum a worthy and potentially fruitful research subject for beam diagnostics.

## THEORETICAL BACKGROUND

TR is generated by a relativistic charge crossing a dielectric interface in a rectilinear and uniform motion [6, 7], in principle. A frequency broad-band photon flux, radiated by the boundary surface around the collision point, propagates towards both the forward and backward half-spaces according to double conical spatial distribution whose angular aperture depends on the Lorentz  $\gamma$  factor of the charge ( $\gamma = E/mc^2$ ). In case of a charge collision at a normal angle of incidence with a flat radiator surface—as also supposed in the following—the angular distribution is symmetric with respect to the motion direction of the charge. As higher and steeper the variation of the dielectric constant across the boundary surface, as larger is the photon yield. Ideal conditions for TR emission are usually encountered in an electron linac beam line where it is produced by a polished metallic foil or a thin Aluminium film on dielectric substrate. As also supposed in the following, for the purposes of the calculation of the transition radiation energy spectrum, the radiator surface can be assimilated to an ideal conductor surface, at least up to the visible spectral region. Under such a hypothesis, for a single electron in collision with an ideal conductor surface, the resultant TR spectrum is uniform in the frequency with angular distribution showing the characteristic double-lobe shape with peak at  $1/\gamma$ . In a electron linac, OTR is mainly observed for monitoring the beam transverse size. Information about the transverse spatial distribution of an electron beam can be obtained by imaging the OTR light spot by means of a CCD camera equipped with a focusing achromatic lens with a focal length  $f$ . A real-size image of the OTR light spot can be obtained for a lens position two times  $f$  equidistant from the image and the object plane. The OTR angular distribution can be instead mapped for a lens distance from the CCD sensor equal to  $f$ . A formal approach to the derivation of the angular distribution of the TR spectra intensity by a relativistic three-dimensional electron beam consists in [3, 4, 5]: (1) calculating the virtual quanta field for the beam [8]; (2) imposing boundary conditions to the transverse harmonic component of the virtual quanta field on the metallic surface; (3) propagating the radiation field from the boundary surface to the observation point by implementing the Helmholtz-Kirchhoff integral theorem; (4) calculating the flux of the Poynting vector; (5) performing the passage from a discrete to a continuous representation of the charge form factors in the radiation energy spectrum provided that the particle density is sufficiently high that the continuous limit can be applied. Highlights of the derivation of the formal expression of the TR energy spectrum by a relativistic electron bunch are below

### New and Emerging Concepts

reported. The following hypothesis will be assumed:  $N$  electrons with spatial coordinates  $[\vec{\rho}_{0j} = (x_{0j}, y_{0j}), z_{0j}]$  ( $j = 1, \dots, N$ ) are supposed to normally hit with a common velocity  $\vec{w} = (0, 0, w)$  a plane metallic surface  $S$  having an arbitrary shape and size and lying on the plane  $z = 0$  of the laboratory frame of reference. According to such a hypothesis, the temporal sequence of the particle collisions with the metallic screen is only a function of the distribution of the electron longitudinal coordinates  $z_{0j}$  ( $j = 1, \dots, N$ ). The formal expression of the transverse harmonic component  $\omega = ck$  of the virtual quanta electric field on the radiator surface  $z = 0$  reads:

$$E_{x,y}^{vq}(x, y, z = 0, \omega) = \frac{ie}{w\pi} \sum_{j=1}^N e^{-i(\omega/w)z_{0j}} \times \int d\vec{\tau} e^{i\vec{\tau} \cdot \vec{\rho}} \frac{\tau_{x,y} e^{-i\vec{\tau} \cdot \vec{\rho}_{0j}}}{\tau^2 + \alpha^2} \quad (1)$$

where  $\vec{\rho} = (x, y)$  and  $\vec{\tau} = (\tau_x, \tau_y)$  are the radiator surface coordinates and conjugate Fourier coordinates, respectively, and  $\alpha = \frac{\omega}{w\gamma}$ . According to the far-field approximation, the Helmholtz-Kirchhoff integral theorem implemented under hypothesis of a radiator surface  $S$  with arbitrary size and shape

$$E_{x,y}^{tr}(\vec{k}, \omega) = \frac{k}{2\pi R} \int_S d\vec{\rho} E_{x,y}^{vq}(\vec{\rho}, \omega) e^{-i\vec{k} \cdot \vec{\rho}} \quad (2)$$

[with  $\vec{k} = (k_x, k_y)$ ] leads to the following formal expression of the TR field at a distance  $R$ :

$$E_{x,y}^{tr}(\vec{k}, \omega) = \sum_{j=1}^N H_{x,y}(\vec{k}, \omega, \vec{\rho}_{0j}) e^{-i(\omega/w)z_{0j}} \quad (3)$$

where  $H_{\mu,j} = H_{\mu}(\vec{k}, \omega, \vec{\rho}_{0j})$  with  $\mu = x, y$

$$H_{\mu,j} = \frac{iek}{2\pi^2 R w} \int_S d\vec{\rho} \int d\vec{\tau} \frac{\tau_{\mu} e^{-i\vec{\tau} \cdot \vec{\rho}_{0j}}}{\tau^2 + \alpha^2} e^{i(\vec{\tau} - \vec{k}) \cdot \vec{\rho}} \quad (4)$$

Finally, by calculating the flux of the Poynting vector, the formal expression of the TR energy spectrum in the most general case of a radiator surface  $S$  having arbitrary size and shape follows:

$$\frac{d^2 I}{d\Omega d\omega} = \frac{cR^2}{4\pi^2} \sum_{\mu=x,y} (\sum_{j=1}^N |H_{\mu,j}|^2 + \sum_{j,l(j \neq l)=1}^N e^{-i(\omega/w)z_{0j}} e^{i(\omega/w)z_{0l}} H_{\mu,j} H_{\mu,l}^*) \quad (5)$$

Some comment about the just obtained results. (1) The formal expression of the TR field—see Eqs.(3,4)—results from the addition of  $N$  single electron field amplitudes  $H_{\mu,j}$ , each depending on the given electron transverse coordinates  $\vec{\rho}_{0j} = (x_{0j}, y_{0j})$  and  $S$ . Furthermore, each field amplitude term shows a relative multiplicative phase factor  $e^{-i(\omega/w)z_{0j}}$  only dependent on the longitudinal coordinate  $z_{0j}$  of the given electron. The relative-phase structure of the radiation field conforms thus to the temporal causality principle that, in the present context, states that

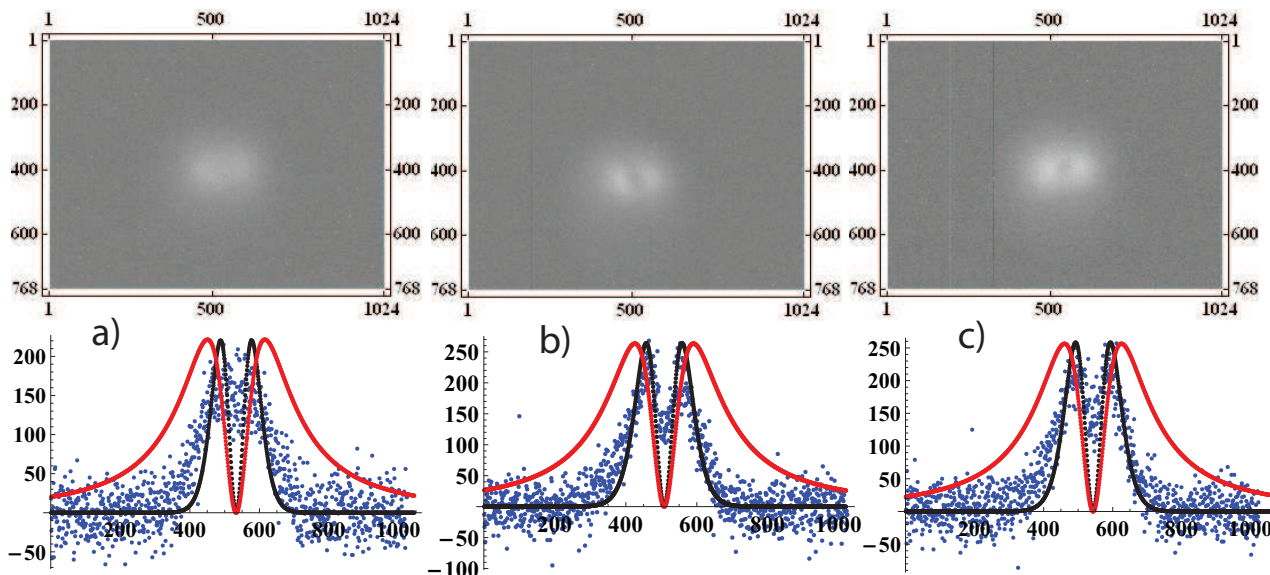


Figure 1: (top) Processed CCD camera images of the OTR angular distribution and (bottom) corresponding radiation intensity distribution along a CCD camera pixel row in comparison with normalized predictions from “single particle” model (red curve) and “beam-transverse-size” model (black curve). The nominal beam transverse size—about 1 mm—decreases passing from a) to b) and c). The fit beam-transverse-size is about 20  $\mu\text{m}$ . One pixel equal to 62  $\mu\text{rad}$ .

the temporal sequence of the particle collision with the radiator surface only depends on the distribution of the electron longitudinal coordinates. (2) The single electron field amplitude—see Eq.(4)—is represented according to an implicit integral formulation—a sort of special function—that in general does not need to be given in an explicit form before the final calculation of the radiation energy spectrum—see Eq.(5)—since both size and shape of the radiator surface  $S$  are, in principle, not *a priori* fixed. (3) Consequently, for the formal derivation of the TR energy spectrum—see Eq.(5)—the implicit representation of Eq.(4) has to be taken into account since the formal expression of the radiation energy spectrum must be independent of the particular shape and size of the radiating screen: in particular, it must be the same whether  $S = \infty$  or  $S < \infty$ . The passage from the discrete—see Eq.(5)—to the continuous limit representation of the radiation energy spectrum can be obtained by averaging Eq.(5) with respect to the distribution function of the particle coordinates. Such an averaging procedure passes through the *ansatz* of the average of the square module of the single particle field amplitude, see Eq.(3,4). Such an *ansatz* can be justified on the basis of the following consideration. The radiation energy spectrum—being the flux of the Poynting vector—is only a dependent function of the radiation field that is the real observable quantity of the electromagnetic radiative mechanism. Consequently, the formal representation in the continuous limit of the radiation energy spectrum must be invariant whether the continuous limit is applied to the flux of the Poynting vector—see Eq.(5)—or directly to the radiation field—see Eqs.(3,4)—prior to the calculation of the flux of the Poynting vector. Moreover, it must be invariant independently of the particular size and shape of the

radiator surface  $S$ . The invariance of the formal representation of the radiation energy spectrum under application of the continuous limit to the flux of the Poynting vector—see Eq.(5)—or to the radiation field—see Eqs.(3,4)—has been already argued in [4]. It should be finally noticed that Eq.(5) can be applied to the description of the TR emission even maintaining the primitive spatial representation of the electron bunch in terms of a discrete particle distribution function. Therefore, all the physical implications of Eq.(5) continue to be valid independently whether the continuous limit is applied or not to the particle density. In conclusion, with reference to [3, 4, 5] for details about the continuous limit and the derivation of the formal results, the expression of OTR energy spectrum—in the present context intended to be the temporal incoherent part of the whole radiation energy spectrum—in the case of a gaussian electron beam with variance  $(\sigma_x, \sigma_y)$  in the transverse plane reads:

$$\frac{d^2I}{d\Omega d\omega} = N \frac{(e\beta)^2}{\pi^2 c} \frac{\sin^2\theta e^{-k^2 \sin^2\theta (\sigma_x^2 \cos^2\phi + \sigma_y^2 \sin^2\phi)}}{(1 - \beta^2 \cos^2\theta)^2} \quad (6)$$

According to Eq.(6), main features of the OTR radiation energy spectrum are: (1) For a given observed wavelength band, the radiated energy increases and its angular distribution broadens with decrease of the beam transverse size. It tends to the angular distribution predicted by the well known “single particle” OTR model for a beam transverse size tending to zero; (2) For a given observed wavelength band and a fixed value of the beam transverse size, the beam-transverse-size model prediction tends to overlap the “single particle” prediction with increase of beam energy. This means that the possible estimate of the beam transverse size from the OTR angular distribution analysis suffers—at high beam energy—from a “saturation” effect that

can be cured by shifting the radiation detection towards the UV part of the visible spectrum.

## EXPERIMENTAL SET-UP

A screen monitor has been set up in the SLS Injector at position SM5 to study properties of OTR, the performance of the imaging system and to test system integration aspects[9]. The particle energy is 100 MeV and the normalized emittance is  $100 \pi$  mm mrad. A quadrupole triplet can be used to focus the beam onto the screen. Three different screens are mounted to the screen ladder: a  $1 \mu\text{m}$  thick titanium foil generating OTR, a cerium doped yttrium aluminum garnet (Ce:YAG) crystal and a cerium doped lutetium aluminum garnet (Ce:LuAG) used as scintillators. All screens are mounted at an angle of  $\pi/4$  to the beam. The screen ladder is inserted by a stepper motor actuator, an absolute encoder verifies the position. The screens are imaged by two cameras, consisting of a 200 and 85 mm lens, respectively, and room-temperature CCD sensors. A third camera is set to image the angular distribution of the light. Beam splitters can be inserted to select the camera. The CCD sensors are digitized with 12-bit accuracy in the cameras. The digital signal is transmitted via a fiber optical link to the computer used for data acquisition. A series of filters can be independently inserted into the optical path: neutral density filters with 1 and 10 % transmission (Kodak Wratten), band-pass filters transmitting the ranges of 380 to 700 nm (B+W 486) and 440 to 500 nm (Roscolux #74), and a long-pass filter with transmission above 590 nm (Roscolux #22).

## EXPERIMENTAL RESULTS

OTR angular distribution has been measured at PSI at the SM5 diagnostic station of the SLS linac for a beam charge of about 0.7 nC and a beam transverse size (RMS) of about 1 mm. In the upper part of Fig.1, several processed images of OTR angular distribution detected by a Point Grey FLEA FL2-08S2M CCD camera (pixel size  $4.65 \mu\text{m}$ ) equipped with a 75 mm focal length objective set at  $\infty$  are shown. They have been obtained by averaging 49 single CCD-camera acquisitions for constant charge and fixed setting of the magnetic optics and then by subtracting the average of an equivalent number of images acquired as background. In the lower part of Fig.1, for each measured OTR angular distribution image, the radiation intensity measured by a single CCD camera pixel row is shown. The given pixel row “cuts” the central part of the OTR light spot along the horizontal direction with respect to the picture, corresponding actually to the vertical transverse axis of the electron beam. The plots of the measured OTR angular distribution along a single pixel row – see Fig.1 a),b) and c) – are compared with normalized numerical curves corresponding to: (red curve) the *single particle model* for OTR, i.e.,  $\sigma_x = \sigma_y = 0$  in Eq.(6); (black curve) the OTR beam-transverse-size model,

i.e.,  $\sigma_x \neq 0, \sigma_y \neq 0$  in Eq.(6). The “black curve” – OTR beam-transverse-size model – has been calculated in the wavelength band  $0.4 \div 0.8 \mu\text{m}$  for a beam transverse size (RMS) between 20 and  $30 \mu\text{m}$ . The analysis of the experimental data in comparison with the single particle and the beam-transverse-size models deserves the following comments: (1) the measured OTR shows the characteristic two-lobe shape with a lobe angular peak position and width shorter and narrower – respectively – than predicted by the single particle model; (2) the observed narrowing of the measured OTR angular distribution is compatible with a diffractive effect that can be described on the basis of the beam-transverse-size model but with a beam transverse size much shorter than what is supposed to be. Further measurements are planned to be performed at PSI for investigating the diffractive effects of the beam-transverse-size on the OTR angular distribution. The OTR beam-transverse-size model has to be improved in order to take into account the full emittance of the beam and the angular tilt of the screen. Improvements in the experimental characterization of the charged beam, in the optical set-up and in the data analysis are also planned.

## CONCLUSION

Measurements of OTR angular distribution at the SLS electron linac are underway at PSI in the framework of the SwissFEL project. Goal of the measurement campaign is to investigate the diffractive effect of the finite beam transverse size on the OTR angular distribution. First results indicate that the OTR single particle model does not fit the data for what concerns both the OTR two lobe angular width and peak position. Evidence of diffractive narrowing of the OTR angular distribution compatible with a finite beam-transverse-size effect has been observed.

## ACKNOWLEDGMENT

The authors wish to acknowledge M. Baldinger, M. Dach, M. Heiniger, A. Kammerer and the SLS operators for precious support.

## REFERENCES

- [1] M. Pedrozzi et al., these proceedings.
- [2] A. Andersson, M. Böge, A. Lüdeke, V. Schlott, A. Streun, Nucl. Instr. and Meth. in Phys. Res. A **591** (2008) 437-446.
- [3] G.L. Orlandi, Opt. Commun. **211** (2002) 109-119.
- [4] G.L. Orlandi, Opt. Commun. **267** (2006) 322-334.
- [5] G.L. Orlandi, EPAC08 Conf. Proc., 1221-1223 (2008).
- [6] V. L. Ginzburg, I. M. Frank, Soviet Phys. JETP **16** (1946) 15.
- [7] M.L. Ter-Mikaelian, *High-Energy Electromagnetic Processes in Condensed Media*, Wiley (1972).
- [8] J.D. Jackson, *Classical Electrodynamics*, Wiley (1975).
- [9] R. Ischebeck, B. Beutner, V. Schlott, B. Steffen, TUPD45 in Proc. DIPAC2009, Basel (2009).